

A Superacid-Catalyzed Synthesis of Porous Membranes Based on Triazine Frameworks for CO₂ Separation

Xiang Zhu,^{†,‡} Chengcheng Tian,^{†,‡} Shannon M. Mahurin,[‡] Song-Hai Chai,[‡] Congmin Wang,^{‡,§} Suree Brown,[#] Gabriel M. Veith,[⊥] Huimin Luo,^{||} Honglai Liu,[†] and Sheng Dai^{*,‡,#}

[†]State Key Laboratory of Chemical Engineering and Department of Chemistry, East China University of Science and Technology, Shanghai 200237, P. R. China

[‡]Chemical Sciences Division, Oak Ridge National Laboratory, Oak Ridge, Tennessee 37831, United States

[§]Department of Chemistry, Zhejiang University, Hangzhou 310027, P. R. China

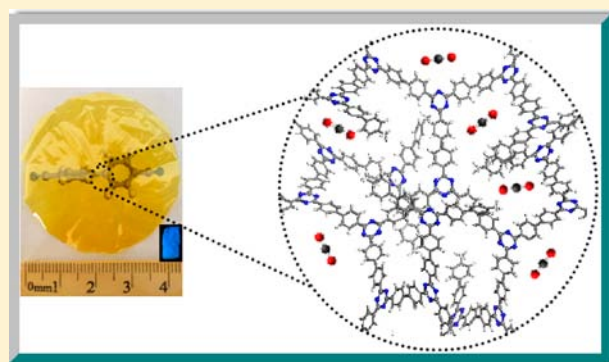
^{||}Nuclear Science and Technology Division, Oak Ridge National Laboratory, Oak Ridge, Tennessee 37831, United States

[⊥]Materials Science and Technology Division, Oak Ridge National Laboratory, Oak Ridge, Tennessee 37831, United States

[#]Department of Chemistry, University of Tennessee, Knoxville, Tennessee 37996-1600, United States

Supporting Information

ABSTRACT: A general strategy for the synthesis of porous, fluorescent, triazine-framework-based membranes with intrinsic porosity through an aromatic nitrile trimerization reaction is presented. The essence of this strategy lies in the use of a superacid to catalyze the cross-linking reaction efficiently at a low temperature, allowing porous polymer membrane architectures to be facilely derived. With functionalized triazine units, the membrane exhibits an increased selectivity for membrane separation of CO₂ over N₂. The good ideal CO₂/N₂ selectivity of 29 ± 2 was achieved with a CO₂ permeability of 518 ± 25 barrer. Through this general synthesis protocol, a new class of porous polymer membranes with tunable functionalities and porosities can be derived, significantly expanding the currently limited library of polymers with intrinsic microporosity for synthesizing functional membranes in separation, catalysis, and energy storage/conversion.



INTRODUCTION

Microporous materials are ubiquitous in various technological and energy-related applications,^{1,2} including gas storage,^{3–10} separations,^{11,12} and catalysis,^{13–17} because of their unique physicochemical properties. Recently, covalently linked microporous organic polymers (MOPs) have attracted considerable attention because their structures and properties can be easily modified through rational chemical design and synthesis. A number of MOPs, including crystalline polymers such as covalent organic frameworks (COFs)^{18,19} and amorphous polymers such as polymers of intrinsic microporosity (PIMs)²⁰ and conjugated microporous polymers (CMPs)^{21–27} have been synthesized through various coupling reactions. Depending on the cavity size and shape, surface area, and regularity, MOPs can be tailored for versatile applications such as membrane-based CO₂ separation. The selective capture and separation of CO₂ using membranes has long been an important area of research because CO₂ is an important greenhouse gas and a renewable carbon source and because membrane technology potentially offers a simple, economical, and energy-efficient method for gas separation.²⁸ Notably, PIMs have emerged as promising membrane materials for CO₂

separation as a result of their good solution processability and special ladder-type structures with contorted sites.^{12,28–44} Continuous research efforts have focused on improving the gas separation ability through increasing the chain rigidity or tuning the cavity size of PIMs. Many CO₂-philic functional groups, such as tetrazole,²⁸ triazine,⁴² and thioamide,³⁹ have been incorporated into the PIMs via postpolymerization of aromatic nitrile groups to improve the separation performance.

Recently, Kuhn and co-workers have developed a new dynamic polymerization system that allows the formation of porous covalent triazine-based frameworks (CTFs) through reversible ionothermal trimerization of nitriles.^{45–48} The condensation reaction is catalyzed by a Lewis acid under conditions of high temperature and autogenic pressure. The derived porous polymers exhibit excellent thermal stabilities as well as highly basic functionalities because of the resulting nitrogen-containing frameworks. However, the key drawback associated with this ionothermal trimerization coupling reaction

Received: February 11, 2012

Revised: May 19, 2012

Published: May 25, 2012

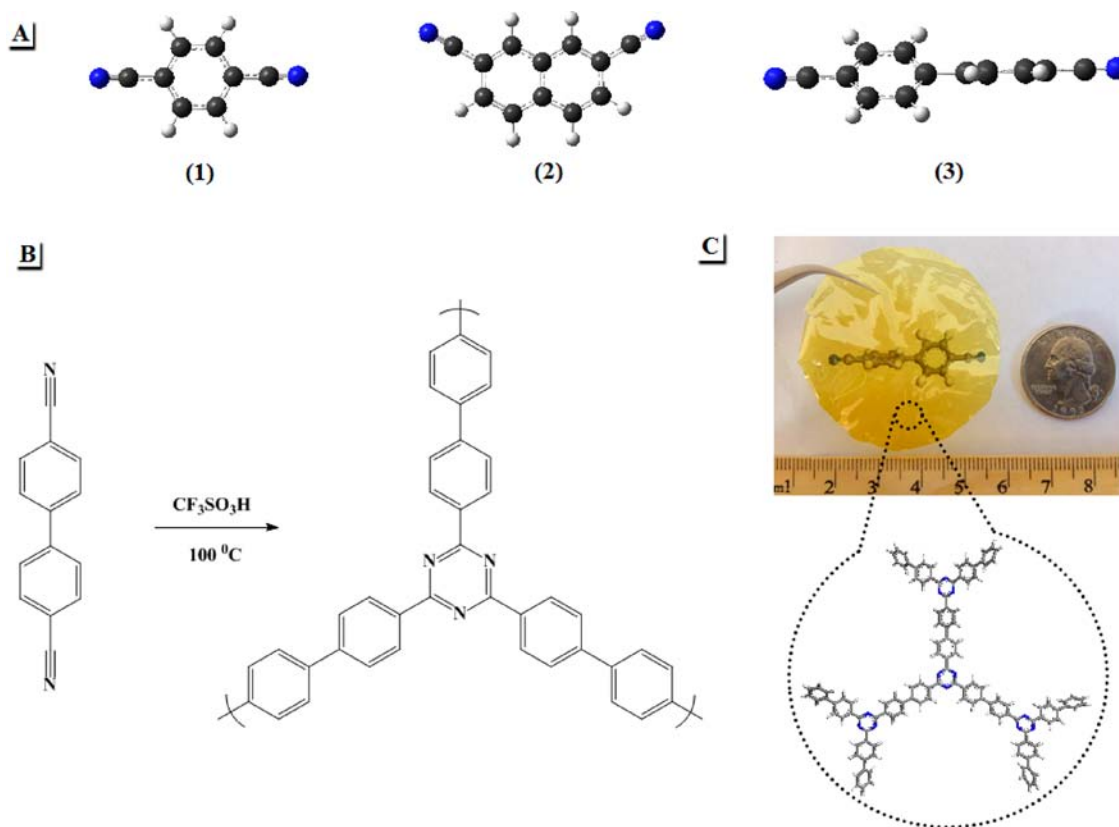


Figure 1. (A) Density functional theory (DFT)-optimized structures of the nitrile monomers used for the membrane synthesis. (B) Trimerization reaction of 4,4'-biphenyldicarbonitrile in $\text{CF}_3\text{SO}_3\text{H}$ at $100\text{ }^\circ\text{C}$. (C) Photograph of a directly synthesized sample of the transparent and flexible triazine-framework-based membrane TFM-1. Inside the circle is shown an “optimized” fragment of the hypothesized framework obtained using Materials Studio (for more details, see the Supporting Information).

is the harsh reaction conditions. Both the high temperature ($\geq 400\text{ }^\circ\text{C}$) and high pressure required for generation of a molten-salt reaction medium (molten ZnCl_2) make the adaptation of this methodology to the synthesis of membranes extremely difficult. Although triazine-based frameworks^{42,49–51} are ideal for the separation of a number of gaseous species from the perspectives of stability and functionality, the above deficiencies hinder the possibility of their effective application as functional membranes in gas separation, catalysis, and energy storage/conversion.

Herein we present a strategy for the direct facile synthesis of triazine-framework-based porous membranes (TFMs) for CO_2 separation through superacid-catalyzed cross-linking reactions at a much lower temperature ($<100\text{ }^\circ\text{C}$). This synthesis strategy was inspired by the discovery that the trimerization reaction of three nitrile groups can be catalytically achieved by a strong protic acid.^{52,53} The essence of this cross-linking reaction strategy lies in its high coupling efficiency and the resultant low-temperature reaction conditions that allow carbon nitrile membranes with intrinsic porosity based on porous triazine frameworks to be successfully prepared, thus considerably expanding the currently limited library of PIMs available for making membranes.^{12,28–37,39–44} Furthermore, our synthesis methodology for polymer membranes is different from more traditional methodologies, which entail the formation of a polymer solution and subsequent solvent evaporation.^{12,30} However, it bears some resemblance to sol–gel processes that entail a polymerization process coupled with concurrent solvent evaporation.

EXPERIMENTAL SECTION

Chemicals. Trifluoromethanesulfonic acid was purchased from Acros. Methanesulfonic acid, sulfuric acid (99.9%), 1,4-dicyanobenzene, and 4,4'-biphenyldicarbonitrile were purchased from Aldrich. 2,7-Naphthalenedicarbonitrile was purchased from TCI America. All were used without further purification.

Synthesis of Membranes. Briefly, 2.5 mL of $\text{CF}_3\text{SO}_3\text{H}$ was added dropwise to 0.5 g of 4,4'-biphenyldicarbonitrile at $-10\text{ }^\circ\text{C}$ under nitrogen in about 3 min. The viscous red solution was stirred for 1.5 h and then poured into a flat glass dish and allowed to spread into a thin layer. With temperature treatment of $100\text{ }^\circ\text{C}$ for ~ 20 min, a soft coating film was successfully formed. The material was then quenched in cold water and washed with diluted NaOH solution for several hours to remove the excess $\text{CF}_3\text{SO}_3\text{H}$. After the material had been washed with water and ethanol several times, the obtained transparent and flexible film was dried in a vacuum oven at $110\text{ }^\circ\text{C}$. The yield was $\sim 80\%$, with the majority of the loss caused by the liquid transfer process. For the synthesis of the other two membranes, derived from 1,4-dicyanobenzene and 2,7-naphthalenedicarbonitrile, a similar reaction temperature and reaction time were used.

CO_2/N_2 Uptake. Gas uptake measurements were obtained using a gravimetric microbalance (Hiden Isochema, IGA) that combines accurate computer control of pressure and temperature with high-precision measurements of sample weight changes to acquire gas uptake isotherms. The sample was loaded into a quartz sample container and sealed in the stainless steel chamber. The sample was dried and degassed at a temperature of $60\text{ }^\circ\text{C}$ and a vacuum pressure of 1 mbar for a minimum of 4 h before the dry mass was recorded. Mass measurements were then acquired at increasing CO_2 pressures up to ~ 1 atm, taking into account the buoyancy effect on the mass. The temperature of the sample was maintained using either a constant-

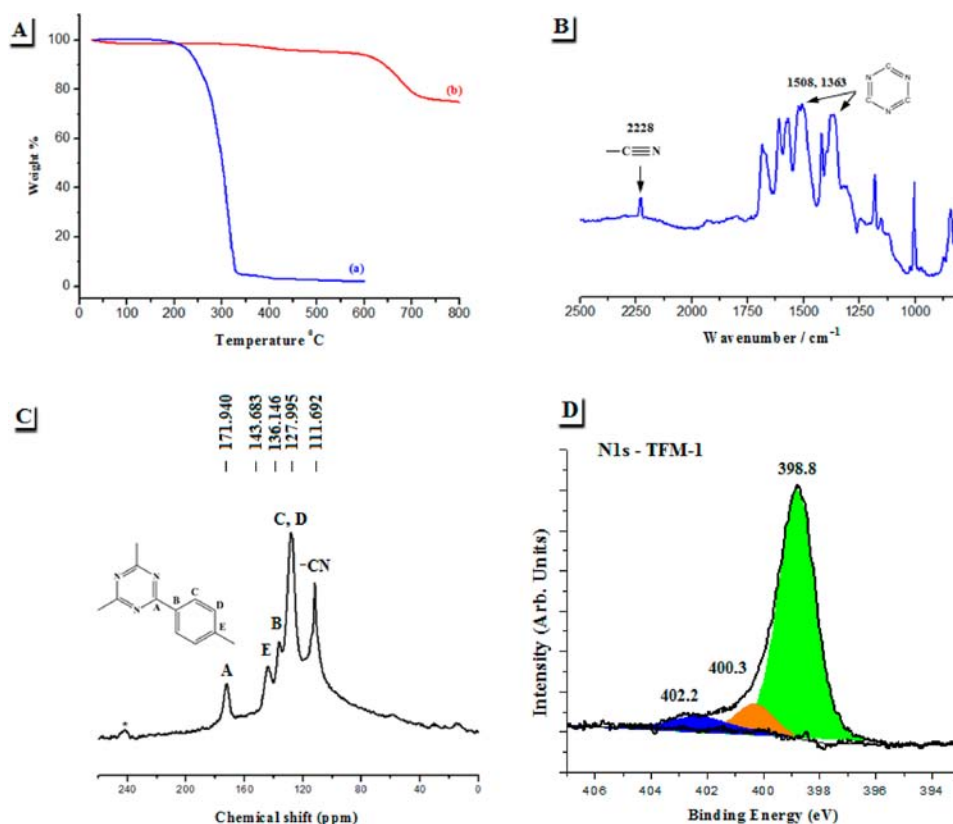


Figure 2. (A) Comparison of the stabilities of (a) the 4,4'-biphenyldicarbonitrile precursor (blue) and (b) the new synthesized membrane TFM-1 (red) under N_2 . (B) FTIR spectrum of TFM-1 prepared at $100\text{ }^\circ\text{C}$. (C) ^{13}C CP-MAS NMR spectrum of TFM-1. (D) Deconvolution of the N 1s peak in the XPS spectrum of TFM-1.

temperature recirculating water bath for the 298 K measurement or an ice bath for the 273 K measurement.

CO_2/N_2 Membrane Separation. Gas permeability measurements were performed using a custom test chamber that has previously been described in detail.⁵⁴ The TFM-1 samples were not large enough to occupy the entire area of the test chamber (47 mm^2), so they were masked by first placing a section of the material on a 47 mm^2 piece of adhesive-backed aluminum with a hole cut in the center. The TFM-1/adhesive aluminum assembly was then attached to a 47 mm^2 aluminum disk ($1/16$ in. thick) whose center was cut with a mating hole corresponding to the hole in the adhesive-backed aluminum, thus creating a sandwich. A thin layer of epoxy was placed on the interface between the TFM-1 and the aluminum to seal the membrane completely and to ensure that the only available diffusion path would be through the membrane. The diameter of the membrane as defined by the holes cut in the center of the aluminum was measured to be 15 mm. The thickness of the membrane was measured using high-resolution calipers. The membrane was then placed in the test chamber and evacuated to ~ 20 mTorr, where it remained overnight. Moreover, before the separation measurement, each side of the TFM-1 membrane was plasma-etched for 10 min to remove any nonporous surface layers and contamination.^{55,56}

Single-gas permeability measurements were performed by isolating the two parts of the chamber (the permeate side and the retentate side) and introducing each gas to the retentate side until a pressure of 35 kPa was reached. The pressure rise on the permeate side was monitored using a 10 Torr Baratron gauge (MKS Instruments) and a data logging program. After an initial delay time corresponding to the time for diffusion through the membrane, the pressure in the permeate side rose linearly with time. From the slope of this pressure rise and the properties of the membrane, the permeability (P) was calculated using the following equation:

$$P = \frac{Vt}{RTA\Delta p} \frac{dp}{dt}$$

where V is the permeate volume, t is the membrane thickness, R is the ideal gas constant, T is the absolute temperature, A is the membrane area, Δp is the pressure difference across the membrane, and dp/dt is the rate of gas pressure increase on the permeate side.

RESULTS AND DISCUSSION

To demonstrate the basic principle regarding the unique advantage of our approach, 4,4'-biphenyldicarbonitrile (**3** in Figure 1A) was selected as the precursor for our membrane synthesis because of the rigid, nonplanar stereochemical arrangement of its two phenyl groups. This precursor was used previously as a monomer in the synthesis of powdered CTFs via a high-temperature trimerization reaction catalyzed by zinc chloride.⁴⁵ Figure 1B provides a schematic representation of the corresponding polymerization process. Instead of zinc chloride, which requires high-temperature ($\geq 400\text{ }^\circ\text{C}$) catalysis and a long reaction time,⁴⁵ the superacid trifluoromethanesulfonic acid ($\text{CF}_3\text{SO}_3\text{H}$)⁵⁷ was applied in our present study to catalyze the cross-linking trimerization reaction at a much lower temperature ($\sim 100\text{ }^\circ\text{C}$) for a shorter time. With this new approach, a transparent, flexible, and thin triazine-framework-based porous membrane, TFM-1, was successfully synthesized (Figure 1C). This new membrane is completely insoluble in common organic solvents such as chloroform and toluene. The superacidity of the catalyst is most likely the main reason that a membrane structure of TFM-1 was obtained rather than a powder morphology as for CTFs. To obtain a better understanding of the importance of the superacid, two

additional strong acids, methanesulfonic acid ($\text{CH}_3\text{SO}_3\text{H}$) and sulfuric acid (H_2SO_4), were used to catalyze the coupling reaction under the same conditions. In contrast to the superacid, no membrane was formed using either of these strong acids under identical reaction conditions. Thus, a superacid catalyst is essential for the effective synthesis of a membrane through efficient low-temperature polymerization of nitrile groups. $\text{CF}_3\text{SO}_3\text{H}$ is considered to be a Brønsted superacid and has a Hammett acidity function (H_0) of -14.1 .⁵⁸ Its acidity is much stronger than those of $\text{CH}_3\text{SO}_3\text{H}$ ($H_0 = -7.86$)⁵⁹ and H_2SO_4 ($H_0 = -12$)⁵⁸ because of the electron-withdrawing fluorine atoms in the sulfonic acid group. Moreover, for the direct synthesis of membranes, solution-processing conditions similar to those for PIM-modified films prepared via the traditional solvent-casting method are usually necessary.^{12,30} Accordingly, our low-temperature solution-based methodology is another key to the successful synthesis of TFM-1. The general synthesis protocol can be used to synthesize other triazine-based membranes.

The polymerization was initially investigated by thermogravimetric analysis (TGA) (Figure 2A). The improved stability of the membrane relative to the precursor, which decomposes or evaporates at ~ 200 °C under N_2 , is consistent with the generation of a rigid polymer framework. The exhibited high thermal stability (Figure S1 in the Supporting Information) is similar to that found for CTFs derived from high-temperature reactions.⁴⁵ It is worth mentioning that the membrane retained its shape after being subjected to thermal annealing at 800 °C under N_2 (Figure S2 in the Supporting Information). The formation of triazine rings inside TFM-1 was indicated by the Fourier-transform IR (FTIR) spectrum (Figure 2B), in which the two strong absorption bands at 1508 and 1363 cm^{-1} represent the aromatic C–N stretching and “breathing” modes in the triazine unit, respectively.⁴⁸ Also, some unreacted terminal nitrile groups were shown by the carbon nitrile band at 2228 cm^{-1} as well.^{45,48} The ^{13}C cross-polarization magic-angle-spinning (CP-MAS) NMR experiment performed on the membrane (Figure 2C) further confirmed the presence of sp^2 carbons from the triazine ring (~ 172 ppm) and the benzene rings (144, 136, 128 ppm) as well as sp carbons from unreacted nitrile groups (112 ppm).⁴⁸ Moreover, the X-ray photoelectron spectroscopy (XPS) data (Figure 2D) support the results obtained by FTIR and NMR spectroscopy. The large N 1s peak centered around 398.8 eV is mainly attributed to the formation of pyridinic nitrogen (C=N–C).^{60–62} This was also well-supported by the C 1s spectrum (Figure S3 in the Supporting Information), which exhibited C–N (286.8 eV) and aromatic carbon (284.8 eV) peaks.⁶³ Furthermore, the energy-dispersive X-ray analysis (EDAX) results (Figure S4 in the Supporting Information) showed that negligible acid impurities existed in the final product, in marked contrast to the final products of the high-temperature process, which are generally contaminated with Zn and Cl ions.⁴⁵

As indicated by the X-ray powder diffraction measurement, our triazine-based framework prepared through the superacid-catalyzed low-temperature reaction was amorphous (Figure S5 in the Supporting Information), indicating less structural order than in crystalline CTFs.^{45,48} Possibly as a result of this amorphous structure, some poorer mechanical properties of TFM-1 were observed in comparison with PIM-1. The tensile strain at break was 9.749% for TFM-1, while the tensile stress at break was 33.1 MPa.³⁸ The pore structure of the networks was evaluated by nitrogen sorption isotherms measured at 77 K

(Figure 3), which revealed TFM-1 to be microporous and exhibit a typical type-I reversible sorption profile. The

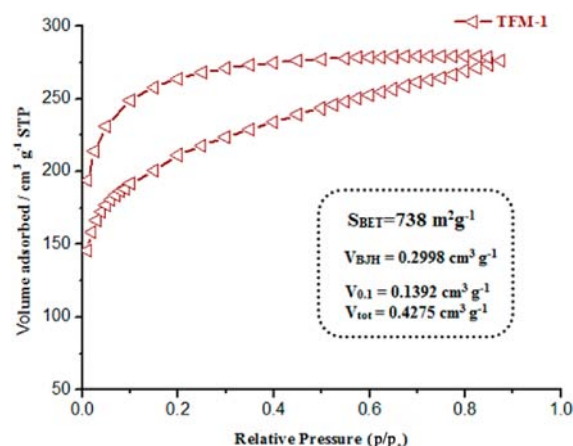


Figure 3. Nitrogen gas adsorption isotherms (measured at 77 K) for TFM-1 condensed at 100 °C in the presence of $\text{CF}_3\text{SO}_3\text{H}$ (V_{tot} is the total volume calculated at $p/p_0 = 0.874$).

Brunauer–Emmett–Teller (BET) surface area (S_{BET}) was ~ 738 m^2 g^{-1} , which is similar to the surface area of 791 m^2 g^{-1} reported for CTF-1 derived from the high-temperature synthesis.⁴⁵ The pore size distribution is shown in Figure S6 in the Supporting Information. The level of microporosity in the materials was assessed by the ratio of micropore volume to the total pore volume ($V_{0.1}/V_{\text{tot}}$).²³ For TFM-1, a $V_{0.1}/V_{\text{tot}}$ value of 0.33 was obtained, indicating the existence of mesopores. The microporosity of TFM-1 should arise simply from the cross-linked triazine polymer, whose highly rigid and contorted molecular structure (Figure 1C) based on the intrinsic structure of 4,4'-biphenyldicarbonitrile (3 in Figure 1A) should prohibit space-efficient packing in the solid state. Accordingly, the generated intrinsic porosity may account for the amorphous structure of TFM-1. To provide a better understanding of the nature of the generated porosity in TFM-1, two additional aromatic nitrile monomers, 1,4-dicyanobenzene and 2,7-naphthalenedicarbonitrile (1 and 2, respectively, in Figure 1A) were selected and polymerized under the same conditions for comparison. The differentiating feature of these two monomers is the lack of any stereochemical repulsion imposed by two adjacent phenyl groups. As a result, no surface area was found for the resulting flexible membranes (Figure S7 in the Supporting Information). This may be due to the planar structures of 1,4-dicyanobenzene and 2,7-naphthalenedicarbonitrile. During the trimerization reaction in $\text{CF}_3\text{SO}_3\text{H}$ at low temperatures, no intrinsic porosity was expected because of the efficient packing of the planar polymer structures. However, it should be noted that significant carbonization was observed for CTFs under ZnCl_2 -catalyzed high-temperature conditions.^{1,48} Accordingly, the observed surface areas for CTFs derived from the high-temperature ionothermal synthesis partially originate from activation processes induced by the molten ZnCl_2 . Moreover, the “optimized” structures of the hypothesized fragments derived from these two precursors through computational modeling (Figure S8 in the Supporting Information) exhibit a planar structure (graphite– C_3N_4 -like)⁶⁵ and can spatially pack efficiently without many stereochemical constraints, leading to their poor porosities. Thus, for the successful synthesis of our porous TFM-1, the intrinsic stereochemical

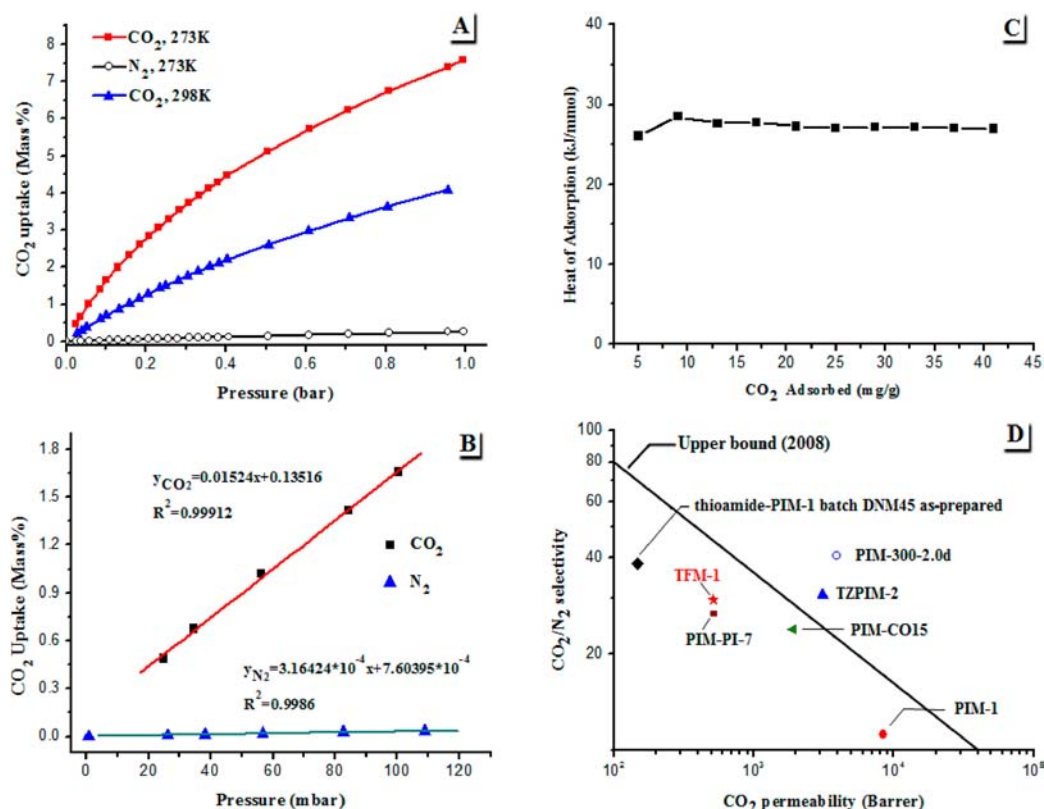


Figure 4. (A) Gas adsorption isotherms of TFM-1 (CO₂ at 273 and 298 K; N₂ at 273 K). (B) Initial slope calculation for CO₂ and N₂ isotherms collected at 273 K. (C) Isosteric heat of adsorption for CO₂ at different CO₂ loadings. (D) Double logarithmic plots of selectivity vs permeability for CO₂/N₂ showing Robeson's 2008 upper bound,⁶⁴ with data for TFM-1 from this work, PIM-1 from Du et al.,³⁵ thioamide-PIM-1 batch DNM45 as-prepared,³⁹ PIM-PI-7,³⁷ tetrazole-functionalized PIM-1 (TZPIM-2),²⁸ thermally self-cross-linked PIM-1 (PIM-300-2.0d),⁴² and PIM-CO15.⁴⁰

structure of the precursor was essential and played a dominant role in determining the porosity of the final membrane.

In view of the intrinsic microporosity, the narrow pore distribution, and the presence of triazine groups inside TFM-1, the CO₂ uptake of TFM-1 was measured up to 1 bar at 273 K and found to be 1.73 mmol g⁻¹ (7.6 mass %; Figure 4A). In comparison, the N₂ uptake of TFM-1 under the same conditions was 0.096 mmol g⁻¹ (0.269 mass %). The estimated CO₂/N₂ adsorption selectivity was 48.2 (Figure 4B). The high selectivity for CO₂ over N₂ can be ascribed to nitrogen sites in the triazine rings, which may facilitate the interaction with the polarizable CO₂ molecules through dipole–quadrupole interactions.⁶⁶ TFM-1 exhibited enhanced CO₂ uptake in comparison with COF-102, even though the latter has a much larger surface area ($S_{\text{BET}} = 3620 \text{ m}^2 \text{ g}^{-1}$, CO₂ uptake = 1.56 mmol g⁻¹).⁶⁷ Therefore, the small pore size and functionality incorporated into TFM-1 play crucial roles in the gas uptake capacity. By fitting the CO₂ adsorption isotherms measured from 0.03 to 1 bar at different temperatures (273 and 298 K) and applying a variant of the Clausius–Clapeyron equation,⁶⁸ we calculated the isosteric heat of adsorption to be in the range 26.1–27.8 kJ mol⁻¹ (Figure 4C), which is comparable to those of some CMP materials (25–33 kJ mol⁻¹).⁵ Notably, unlike other powder MOPs such as COFs and CMPs, membrane separation measurements on TFM-1 could be carried out successfully. The gas separation capabilities of the membrane were examined using a non-steady-state permeation cell at 298 K. The pressure difference was 0.35 bar. Permeability values for CO₂ and N₂ were separately measured through the membrane, and ideal CO₂/N₂ selectivity values

were calculated. Moreover, the diffusion coefficient (D) and solubility coefficient (S), which are related to the permeability by the expression $P = SD$, were measured for CO₂ by the time-lag permeation method. The CO₂ permeability and CO₂/N₂ selectivity were measured to be 518 ± 25 barrer and 29 ± 2 , respectively. A plot of selectivity versus permeability, generally called a Robeson plot, is shown in Figure 4D. Although TFM-1 has a surface area similar to that of PIM-1 ($S_{\text{BET}} \approx 700 \text{ m}^2 \text{ g}^{-1}$), the amount of CO₂ absorbed by TFM-1 at 273 K (Figure 4A) is much smaller than that adsorbed by PIM-1 in the low-pressure range,²⁸ which may explain the reduction of the permeability coefficient. On the basis of the possible dipole–quadrupole interactions between the nitrogen sites of triazine rings and CO₂ molecules,⁶⁶ the incorporation of basic triazine groups into the rigid framework may enhance the selectivity for CO₂ over N₂, indicating a considerably higher ideal selectivity than for PIM-1. Moreover, the diffusion and solubility coefficients were smaller than that of PIM-1 and shown to be $2.4 \times 10^{-7} \text{ cm}^2 \text{ s}^{-1}$ and $21.6 \times 10^{-2} \text{ cm}^3 / (\text{cm}^3 \text{ cmHg}^{-1})$,²⁹ respectively. It is worth mentioning that similar gas separation performances of thioamide-PIM-1 (DNM45) before ethanol treatment and PIM-PI-7 have been investigated.^{37,39} High selectivity can be more important than high permeability because membrane module design or process design can never improve a low selectivity, whereas a low permeability can be overcome.³⁹

Furthermore, unlike black CTFs, the TFM-1 membranes are yellow in color and show blue fluorescence with a maximum emission at $\sim 440 \text{ nm}$ under excitation at 340 nm, as shown by the photoluminescence spectrum in Figure 5. A relatively broad

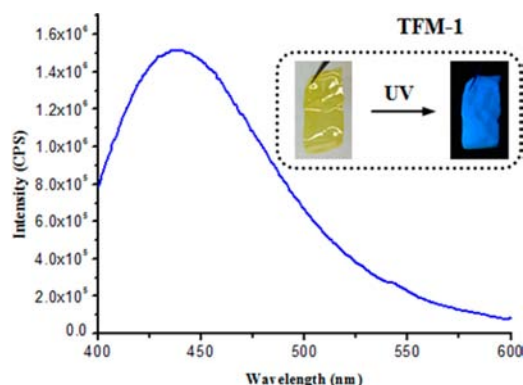


Figure 5. Photoluminescence spectrum of TFM-1. The inset shows the different colors of TFM-1 before and after excitation under UV light.

absorption was observed in the solid-state UV–vis spectrum as well (Figure S9 in the Supporting Information). Therefore, on the basis of the strong electron-accepting ability and high symmetry of the triazine units, the photophysical properties of TFM-1 membrane suggest potential optoelectronic applications.⁶⁹

CONCLUSIONS

In summary, we have developed a general method for the direct and facile synthesis of a porous, fluorescent triazine-framework-based membrane through a low-temperature reaction (<100 °C) in the presence of a superacid (CF₃SO₃H). TFM-1 was shown to be intrinsically microporous, with a high BET surface area of 738 m² g⁻¹, as a result of the rigid and intrinsic spatial structure of 4,4'-biphenyldicarbonitrile. At 273 K and 1 bar, TFM-1 exhibited a good CO₂ uptake of 1.73 mmol g⁻¹. Furthermore, with functionalized triazine units, the membrane exhibits increased selectivity for the membrane separation of CO₂ over N₂. An ideal CO₂/N₂ permselectivity of 29 ± 2 was achieved, with a CO₂ permeability of 518 ± 25 barrer. With our synthesis method, the solubility of the resulting microporous organic polymers is no longer the constraining factor in the synthesis of highly cross-linked polymer membranes. We believe that a number of new microporous polymer membranes can be readily prepared from abundant aromatic nitrile compounds using our general synthesis protocol.

ASSOCIATED CONTENT

Supporting Information

Details of experimental procedures, quantum-chemical calculations, and framework optimization and Figures S1–S9. This material is available free of charge via the Internet at <http://pubs.acs.org>.

AUTHOR INFORMATION

Corresponding Author

dais@ornl.gov

Notes

The authors declare no competing financial interest. After initial submission of this paper as a communication (Feb. 2, 2012), another communication (DOI: 10.1002/adma.201200751) on the synthesis of powdered triazine frameworks by the strong Bronsted acid was submitted by A. I. Cooper and his coworkers to *Advanced Materials* on Feb. 21, 2012 and published online on April 4, 2012.

ACKNOWLEDGMENTS

X.Z. and C.C.T. were financially supported by the U.S. Department of Energy, Advanced Research Projects Agency-ENERGY. C.W., S.M.M., S.H.-C., S.B., H.M.L., and S.D. were sponsored by the Division of Chemical Sciences, Geosciences, and Biosciences, Office of Basic Energy Sciences, U.S. Department of Energy. G.M.V. was supported by the U.S. Department of Energy, Office of Basic Energy Sciences, Division of Materials Sciences and Engineering. X.Z. and H.L.L. acknowledge the support from National Natural Science Foundation of China (No. 20990224, 21076071), the National High Technology Research and Development Program of China (No. 2008AA062302), the 111 Project of China (No.B08021), and the Fundamental Research Funds for the Central Universities of China.

REFERENCES

- (1) Dawson, R.; Cooper, A. I.; Adams, D. J. *Prog. Polym. Sci.* **2012**, *37*, 530.
- (2) McKeown, N. B.; Budd, P. M. *Macromolecules* **2010**, *43*, 5163.
- (3) Svec, F.; Germain, J.; Fréchet, J. M. J. *Small* **2009**, *5*, 1098.
- (4) Eddaoudi, M.; Kim, J.; Rosi, N.; Vodak, D.; Wachter, J.; O'Keeffe, M.; Yaghi, O. M. *Science* **2002**, *295*, 469.
- (5) Dawson, R.; Stockel, E.; Holst, J. R.; Adams, D. J.; Cooper, A. I. *Energy Environ. Sci.* **2011**, *4*, 4239.
- (6) Farha, O. K.; Spokoyny, A. M.; Hauser, B. G.; Bae, Y.-S.; Brown, S. E.; Snurr, R. Q.; Mirkin, C. A.; Hupp, J. T. *Chem. Mater.* **2009**, *21*, 3033.
- (7) Farha, O. K.; Bae, Y.-S.; Hauser, B. G.; Spokoyny, A. M.; Snurr, R. Q.; Mirkin, C. A.; Hupp, J. T. *Chem. Commun.* **2010**, *46*, 1056.
- (8) Lu, W.; Yuan, D.; Sculley, J.; Zhao, D.; Krishna, R.; Zhou, H.-C. *J. Am. Chem. Soc.* **2011**, *133*, 18126.
- (9) He, Y.; Xiang, S.; Chen, B. *J. Am. Chem. Soc.* **2011**, *133*, 14570.
- (10) Ben, T.; Ren, H.; Ma, S.; Cao, D.; Lan, J.; Jing, X.; Wang, W.; Xu, J.; Deng, F.; Simmons, J. M.; Qiu, S.; Zhu, G. *Angew. Chem., Int. Ed.* **2009**, *48*, 9457.
- (11) Kuhn, P.; Kruger, K.; Thomas, A.; Antonietti, M. *Chem. Commun.* **2008**, 5815.
- (12) McKeown, N. B.; Budd, P. M. *Chem. Soc. Rev.* **2006**, *35*, 675.
- (13) Kaur, P.; Hupp, J. T.; Nguyen, S. T. *ACS Catal.* **2011**, *1*, 819.
- (14) Chen, L.; Yang, Y.; Jiang, D. *J. Am. Chem. Soc.* **2010**, *132*, 9138.
- (15) Xie, Z.; Wang, C.; deKrafft, K. E.; Lin, W. *J. Am. Chem. Soc.* **2011**, *133*, 2056.
- (16) Jiang, J.-X.; Wang, C.; Laybourn, A.; Hasell, T.; Clowes, R.; Khimiyak, Y. Z.; Xiao, J.; Higgins, S. J.; Adams, D. J.; Cooper, A. I. *Angew. Chem., Int. Ed.* **2011**, *50*, 1072.
- (17) Rose, M.; Notzon, A.; Heitbaum, M.; Nickerl, G.; Paasch, S.; Brunner, E.; Glorius, F.; Kaskel, S. *Chem. Commun.* **2011**, *47*, 4814.
- (18) Côté, A. P.; Benin, A. I.; Ockwig, N. W.; O'Keeffe, M.; Matzger, A. J.; Yaghi, O. M. *Science* **2005**, *310*, 1166.
- (19) El-Kaderi, H. M.; Hunt, J. R.; Mendoza-Cortés, J. L.; Côté, A. P.; Taylor, R. E.; O'Keeffe, M.; Yaghi, O. M. *Science* **2007**, *316*, 268.
- (20) Budd, P. M.; Ghanem, B. S.; Makhseed, S.; McKeown, N. B.; Msayib, K. J.; Tattershall, C. E. *Chem. Commun.* **2004**, 230.
- (21) Jiang, J. X.; Su, F.; Trewin, A.; Wood, C. D.; Campbell, N. L.; Niu, H.; Dickinson, C.; Ganin, A. Y.; Rosseinsky, M. J.; Khimiyak, Y. Z.; Cooper, A. I. *Angew. Chem., Int. Ed.* **2008**, *47*, 1167.
- (22) Cooper, A. I. *Adv. Mater.* **2009**, *21*, 1291.
- (23) Dawson, R.; Laybourn, A.; Clowes, R.; Khimiyak, Y. Z.; Adams, D. J.; Cooper, A. I. *Macromolecules* **2009**, *42*, 8809.
- (24) Holst, J. R.; Stoeckel, E.; Adams, D. J.; Cooper, A. I. *Macromolecules* **2010**, *43*, 8531.
- (25) Xu, Y.; Chen, L.; Guo, Z.; Nagai, A.; Jiang, D. *J. Am. Chem. Soc.* **2011**, *133*, 17622.
- (26) Kou, Y.; Xu, Y.; Guo, Z.; Jiang, D. *Angew. Chem., Int. Ed.* **2011**, *50*, 8753.

- (27) Mohanty, P.; Kull, L. D.; Landskron, K. *Nat. Commun.* **2011**, *2*, 401.
- (28) Du, N.; Park, H. B.; Robertson, G. P.; Dal-Cin, M. M.; Visser, T.; Scoles, L.; Guiver, M. D. *Nat. Mater.* **2011**, *10*, 372.
- (29) Budd, P. M.; Msayib, K. J.; Tattershall, C. E.; Ghanem, B. S.; Reynolds, K. J.; McKeown, N. B.; Fritsch, D. *J. Membr. Sci.* **2005**, *251*, 263.
- (30) McKeown, N. B.; Budd, P. M.; Msayib, K. J.; Ghanem, B. S.; Kingston, H. J.; Tattershall, C. E.; Makhseed, S.; Reynolds, K. J.; Fritsch, D. *Chem.—Eur. J.* **2005**, *11*, 2610.
- (31) Ghanem, B. S.; McKeown, N. B.; Budd, P. M.; Selbie, J. D.; Fritsch, D. *Adv. Mater.* **2008**, *20*, 2766.
- (32) Staiger, C. L.; Pas, S. J.; Hill, A. J.; Cornelius, C. J. *Chem. Mater.* **2008**, *20*, 2606.
- (33) Budd, P. M.; McKeown, N. B. *Polym. Chem.* **2010**, *1*, 63.
- (34) Du, N.; Robertson, G. P.; Song, J.; Pinnau, I.; Thomas, S.; Guiver, M. D. *Macromolecules* **2008**, *41*, 9656.
- (35) Du, N.; Robertson, G. P.; Song, J.; Pinnau, I.; Guiver, M. D. *Macromolecules* **2009**, *42*, 6038.
- (36) Du, N.; Robertson, G. P.; Pinnau, I.; Guiver, M. D. *Macromolecules* **2009**, *42*, 6023.
- (37) Ghanem, B. S.; McKeown, N. B.; Budd, P. M.; Al-Harbi, N. M.; Fritsch, D.; Heinrich, K.; Starannikova, L.; Tokarev, A.; Yampolskii, Y. *Macromolecules* **2009**, *42*, 7881.
- (38) Du, N.; Robertson, G. P.; Pinnau, I.; Guiver, M. D. *Macromolecules* **2010**, *43*, 8580.
- (39) Mason, C. R.; Maynard-Atem, L.; Al-Harbi, N. M.; Budd, P. M.; Bernardo, P.; Bazzarelli, F.; Clarizia, G.; Jansen, J. C. *Macromolecules* **2011**, *44*, 6471.
- (40) Fritsch, D.; Bengtson, G.; Carta, M.; McKeown, N. B. *Macromol. Chem. Phys.* **2011**, *212*, 1137.
- (41) Du, N.; Cin, M. M. D.; Pinnau, I.; Nicalek, A.; Robertson, G. P.; Guiver, M. D. *Macromol. Rapid Commun.* **2011**, *32*, 631.
- (42) Li, F. Y.; Xiao, Y.; Chung, T.-S.; Kawi, S. *Macromolecules* **2012**, *45*, 1427.
- (43) Ma, X.; Swaidan, R.; Belmabkhout, Y.; Zhu, Y.; Litwiller, E.; Jouiad, M.; Pinnau, I.; Han, Y. *Macromolecules* **2012**, *45*, 3841.
- (44) Du, N.; Park, H. B.; Dal-Cin, M. M.; Guiver, M. D. *Energy Environ. Sci.* **2012**, *5*, 7306.
- (45) Kuhn, P.; Antonietti, M.; Thomas, A. *Angew. Chem., Int. Ed.* **2008**, *47*, 3450.
- (46) Kuhn, P.; Forget, A.; Su, D.; Thomas, A.; Antonietti, M. *J. Am. Chem. Soc.* **2008**, *130*, 13333.
- (47) Kuhn, P.; Thomas, A.; Antonietti, M. *Macromolecules* **2009**, *42*, 319.
- (48) Bojdys, M. J.; Jeromenok, J.; Thomas, A.; Antonietti, M. *Adv. Mater.* **2010**, *22*, 2202.
- (49) Schwab, M. G.; Fassbender, B.; Spiess, H. W.; Thomas, A.; Feng, X.; Müllen, K. *J. Am. Chem. Soc.* **2009**, *131*, 7216.
- (50) Chan-Thaw, C. E.; Villa, A.; Katekomol, P.; Su, D.; Thomas, A.; Prati, L. *Nano Lett.* **2010**, *10*, 537.
- (51) Ren, H.; Ben, T.; Wang, E.; Jing, X.; Xue, M.; Liu, B.; Cui, Y.; Qiu, S.; Zhu, G. *Chem. Commun.* **2010**, *46*, 291.
- (52) Hayami, S.; Inoue, K. *Chem. Lett.* **1999**, 545.
- (53) Yasuda, T.; Shimizu, T.; Liu, F.; Ungar, G.; Kato, T. *J. Am. Chem. Soc.* **2011**, *133*, 13437.
- (54) Mahurin, S. M.; Lee, J. S.; Wang, X.; Dai, S. *J. Membr. Sci.* **2011**, *368*, 41.
- (55) Vandezande, P.; Gevers, L. E. M.; Vankelecom, I. F. J. *Chem. Soc. Rev.* **2008**, *37*, 365.
- (56) Wang, X.; Zhu, Q.; Mahurin, S. M.; Liang, C.; Dai, S. *Carbon* **2010**, *48*, 557.
- (57) Olah, G. A.; Klumpp, D. A. *Acc. Chem. Res.* **2004**, *37*, 211.
- (58) Angueira, E. J.; White, M. G. *J. Mol. Catal. A: Chem.* **2007**, *277*, 164.
- (59) Bascombe, K. N.; Bell, R. P. *J. Chem. Soc.* **1959**, 1096.
- (60) Thomas, A.; Fischer, A.; Goettmann, F.; Antonietti, M.; Müller, J.-O.; Schlogl, R.; Carlsson, J. M. *J. Mater. Chem.* **2008**, *18*, 4893.
- (61) Luo, Z.; Lim, S.; Tian, Z.; Shang, J.; Lai, L.; MacDonald, B.; Fu, C.; Shen, Z.; Yu, T.; Lin, J. *J. Mater. Chem.* **2011**, *21*, 8038.
- (62) Khabashesku, V. N.; Zimmerman, J. L.; Margrave, J. L. *Chem. Mater.* **2000**, *12*, 3264.
- (63) Parakwitsch, J. P.; Thomas, A.; Antonietti, M. *J. Mater. Chem.* **2010**, *20*, 6746.
- (64) Robeson, L. M. *J. Membr. Sci.* **2008**, *320*, 390.
- (65) Wang, X.; Maeda, K.; Thomas, A.; Takanabe, K.; Xin, G.; Carlsson, J. M.; Domen, K.; Antonietti, M. *Nat. Mater.* **2009**, *8*, 76.
- (66) Rabbani, M. G.; El-Kaderi, H. M. *Chem. Mater.* **2011**, *23*, 1650.
- (67) Furukawa, H.; Yaghi, O. M. *J. Am. Chem. Soc.* **2009**, *131*, 8875.
- (68) Chen, Q.; Luo, M.; Hammershøj, P.; Zhou, D.; Han, Y.; Laursen, B. W.; Yan, C.-G.; Han, B.-H. *J. Am. Chem. Soc.* **2012**, *134*, 6084.
- (69) Omer, K. M.; Ku, S.-Y.; Chen, Y.-C.; Wong, K.-T.; Bard, A. J. *J. Am. Chem. Soc.* **2010**, *132*, 10944.